Annual Review of Virology

The Hepatitis B Virus Envelope Proteins: Molecular Gymnastics Throughout the Viral Life Cycle

Stefan Seitz,[1] Jelena Habjanič,[2,3] Anne K. Schütz,[2,3] and Ralf Bartenschlager[1,4]

[1]Department of Infectious Diseases, University of Heidelberg, 69120 Heidelberg, Germany; email: ralf.bartenschlager@med.uni-heidelberg.de

[2]Bavarian NMR Center, Department of Chemistry, Technical University of Munich, 85748 Garching, Germany

[3]Institute of Structural Biology, Helmholtz Zentrum München, 85764 Neuherberg, Germany

[4]Division of Virus-Associated Carcinogenesis, German Cancer Research Center (DKFZ), 69120 Heidelberg, Germany

Annu. Rev. Virol. 2020. 7:22.1–22.26

The *Annual Review of Virology* is online at virology.annualreviews.org

https://doi.org/10.1146/annurev-virology-092818-015508

Keywords

Dane particle, virion maturation, nucleocapsid, membrane protein, topological switch, maturation signal, post-translational modification, glycosylation, electron microscopy

Abstract

New hepatitis B virions released from infected hepatocytes are the result of an intricate maturation process that starts with the formation of the nucleocapsid providing a confined space where the viral DNA genome is synthesized via reverse transcription. Virion assembly is finalized by the enclosure of the icosahedral nucleocapsid within a heterogeneous envelope. The latter contains integral membrane proteins of three sizes, collectively known as hepatitis B surface antigen, and adopts multiple conformations in the course of the viral life cycle. The nucleocapsid conformation depends on the reverse transcription status of the genome, which in turn controls nucleocapsid interaction with the envelope proteins for virus exit. In addition, after secretion the virions undergo a distinct maturation step during which a topological switch of the large envelope protein confers infectivity. Here we review molecular determinants for envelopment and models that postulate molecular signals encoded in the capsid scaffold conducive or adverse to the recruitment of envelope proteins.

INTRODUCTION

Infections with the human hepatitis B virus (HBV) are a health burden of global importance (1) with at least 257 million people being chronic virus carriers. About 890,000 individuals die each year due to HBV-driven liver diseases, including liver cirrhosis and hepatocellular carcinoma (2). HBV belongs to the large and ancient family *Hepadnaviridae*, members of which are found in all bony vertebrate classes. These viruses coevolved in intimate association with their hosts over several hundred million years, which explains their success in establishing persistent infections (3–5).

The hepatitis B virion, termed Dane particle after its discoverer, appears as a double-shelled spherical particle ∼42 nm in diameter (**Figure 1*a*,*b***) (6). Its central structure is an icosahedral capsid that is built from core (C) protein and harbors a circular, partially double-stranded DNA (dsDNA) genome together with the viral polymerase P. This nucleocapsid is surrounded by a lipid envelope into which the surface glycoproteins L (large), M (middle), and S (small) are embedded. Subviral particles (SVP) of spherical and filamentous shape are composed of empty envelopes and outnumber virions by 10^3-fold to 10^6-fold, both in vivo and in cell culture (7).

The reverse-transcribed DNA genome of HBV is tiny, comprising ∼3.2 kb, and is characterized by an extreme utilization of gene overlap (**Figure 1*c***). Each nucleotide participates in protein coding, and about half of them participate in double-coding two proteins. Consequently, all *cis*-acting elements are part of at least one open reading frame (ORF). In a linear array, the total informational content would roughly correspond to 7.5 kb. In a figurative sense, the HBV genome resembles a ZIP-compressed file of a conventional retroviral genome. Thus, we consider it as the most highly evolved genome on earth.

The evolutionary constraint creating this condensed organization is imposed by the peculiar replication mechanism of HBV. Reverse transcription of the pregenomic RNA (pgRNA) template by P is a multistep process involving several template switches during minus- and plus-strand DNA synthesis (8), yet it entirely takes place cytosolically inside the viral capsid, i.e., a spatially highly restricted compartment (step 1 in **Figure 1*d***). Upon progress of dsDNA synthesis, nucleocapsids gain competence to interact with the viral surface glycoproteins to become enveloped and secreted as complete virions into the lumen of multivesicular bodies (9). The aim of our review is to provide an overview of available literature about the interactions between all molecular players involved and the series of accompanying structural changes that occur before, during, and after envelopment. We put a focus on the maturation of the envelope glycoproteins and their interaction with nucleocapsids and devise a hypothetical model for the series of events (**Figure 1*d***). We regard the HBV Dane particle as an effective nanomachine in which several concentric shells are highly interconnected and changes in any zone might trigger secondary changes in the neighboring zone.

HEPATITIS B VIRUS CAPSID STRUCTURE AND ITS DYNAMICS

The HBV capsid protein C (HBc) comprises 183 amino acids (aa) and is divided into two functionally distinct domains connected via a linker (**Figure 2*a***). The N-terminal domain (NTD, aa1–140) mediates assembly and forms the scaffold of the capsid shell. The highly basic, arginine-rich C-terminal domain (CTD, aa149–183) functions in nucleic acid binding and incorporation of the viral replication complex. The NTD adopts a fold with five α-helices (α1–α5) connected by short loops (10). C monomers associate into homodimers of inverted T shape via interaction of two NTDs, each contributing an α-helical hairpin (α3/α4), creating a four-helix bundle (**Figure 2*b***).

In vivo and in vitro, C dimers self-assemble into capsid particles of spherical appearance with a holey shell and protruding spikes formed by the four-helix bundles (10–13) (**Figure 2*c***). Assembly

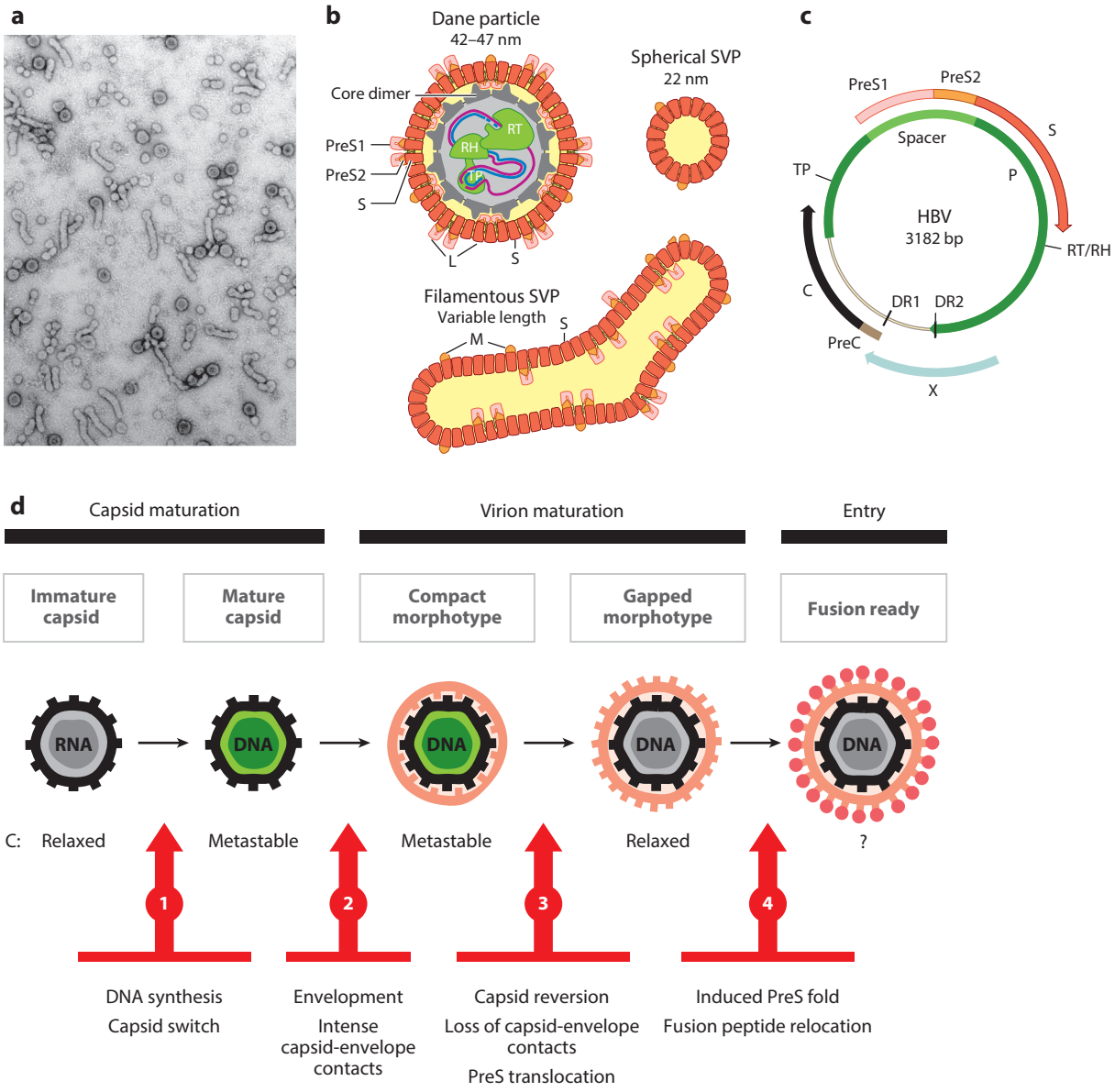

Figure 1

HBV particle and genome architecture and model of HBV maturation. (*a*) Transmission electron micrograph of HBV particles purified from serum of a chronic patient. (*b*) Schematic of the particle architecture of virions and SVP. (*c*) HBV genome map. (*d*) Model of the maturation steps. Abbreviations: C, core; DR, direct repeat; HBV, hepatitis B virus; L, large; M, middle; P, polymerase; PreC, Precore; RH, RNase H; RT, reverse transcriptase; S, small; SVP, subviral particles; TP, terminal protein; X, X gene.

upon expression of C1–149 in *Escherichia coli* is efficient without viral nucleic acid (**Figure 2*a***). The interaction between the CTD of full-length C and short stem-loop structures scattered along the pgRNA strongly drives assembly of nucleocapsids enclosing authentic replication complexes (14). The vast majority of capsids exhibit a diameter of ~34 nm and are composed of 120 C

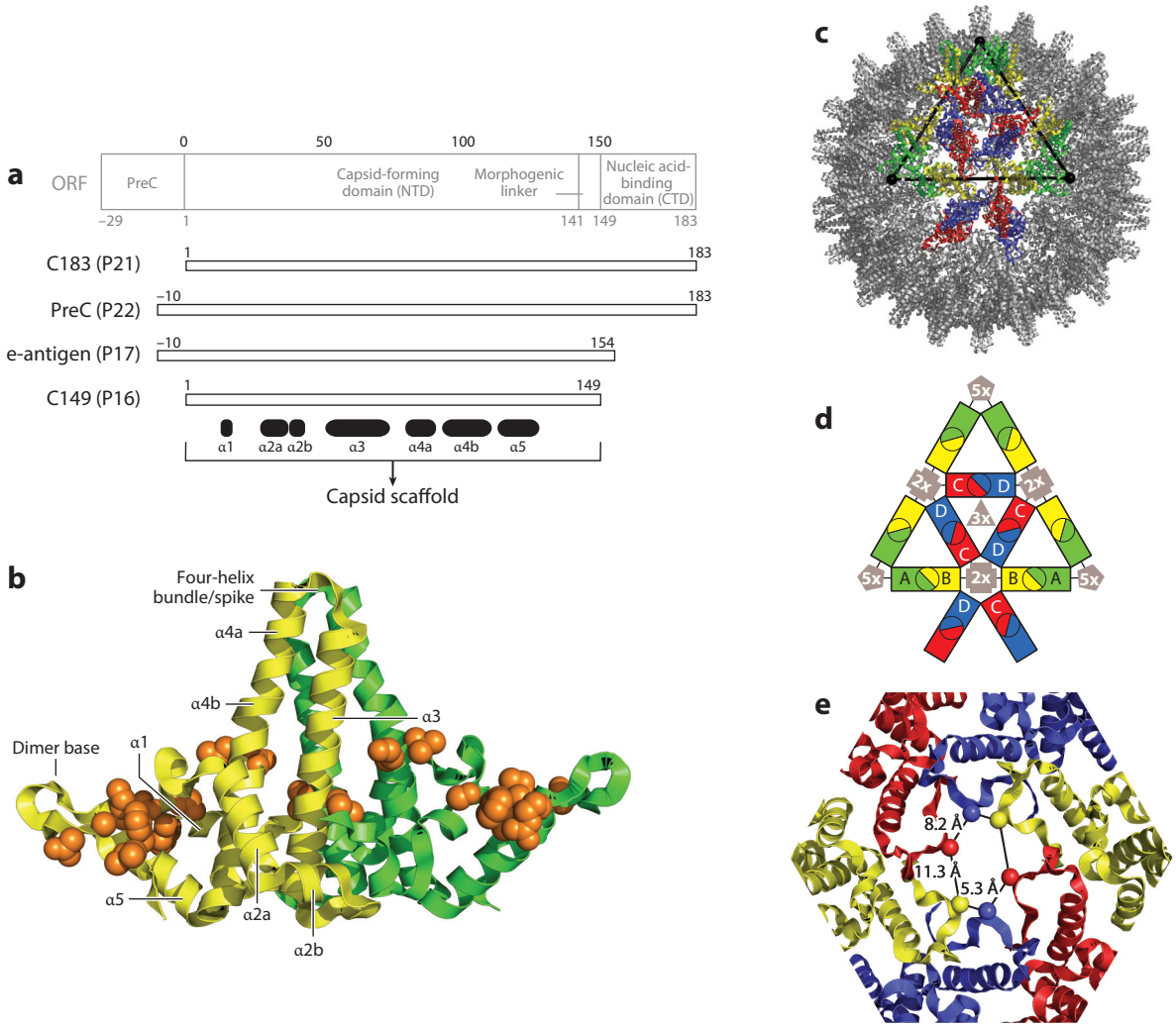

Figure 2

Primary to quaternary architecture of HBc. (*a*) The PreC/C ORF and the protein variants that result from differential translation initiation and proteolytic processing. The C protein is synthesized by translation initiation at an internal AUG codon (position 1 by definition). The PreC precursor protein is synthesized by translation initiation at the upstream AUG codon (position −29). The N-terminal 19 aa act as a signal peptide mediating SRP-dependent translocation into the ER lumen. Subsequent cleavage of the signal peptide gives rise to the PreC protein (P22), which is further converted into the secreted e-antigen by furin cleavage in the C-terminal region in a post-ER compartment. The monomeric subunits of C and the e-antigen are very similar in their fold, but homodimerization occurs via different interfaces. The position of helices in NTD is indicated by black tubes. (*b*) Side view of the NTD dimer in ribbon-style representation (PDB 1qgt). aa residues whose mutation affects capsid envelopment but not assembly are shown as orange spheres (132). (*c*) Representation of the icosahedral $T = 4$ capsid (PDB 1qgt) with the C subunits highlighted in color corresponding to the scheme shown in subpanel *d*. One triangular icosahedron face is highlighted in black. (*d*) Scheme of the C protein dimer arrangement in the $T = 4$ capsid architecture. Quasiequivalent C subunits in the asymmetric unit are color coded and labeled from A to D by convention. The icosahedral symmetry axes are symbolized in gray. The capsid spike sits at local twofold axes, indicated by circles. The base of the dimers forms interdimer contacts. (*e*) Zoom of the twofold (pseudo-sixfold) axis. Distances between Pro135 Cβ atoms in quasiequivalent subunits are indicated. Abbreviations, aa, amino acid; ER, endoplasmic reticulum; HBc, hepatitis B virus core protein C; NTD, N-terminal domain; ORF, open reading frame; PDB, Protein Databank; PreC, Precore; SRP, signal recognition particle.

dimers arranged with icosahedral symmetry of triangulation $T = 4$ (15). A minor fraction (~5%) is smaller (~30 nm), composed of 90 dimers displaying triangulation icosahedral symmetry with $T = 3$. The four C subunits representing the asymmetric unit in $T = 4$ capsids are labeled from A to D (**Figure 2*d***) (10). AB-dimers meet at the icosahedral fivefold axes by interdimer contacts between A subunits. Three CD-dimers interact around the threefold axes. At the twofold axes, four CD- and two AB-dimers come together, creating a pseudo-sixfold environment (**Figure 2*c,d***). The quasiequivalent nature of the icosahedral array is exemplified best in this region by the different extents of the interdimer contacts, which result in different distances between quasiequivalent marker atoms (**Figure 2*e***). While the B-on-D interdimer contact appears most intense, the C-on-B contact is the loosest. Because the interdimer contacts are weak (16), one can easily envisage conformational changes, e.g., switches in the intensities of the interdimer contacts, to occur upon encapsidation of the replication complex (14, 17), reverse transcription of the genome (18), and envelopment and virion secretion, but also during later steps priming the release of nucleocapsids into the host cell. Indeed, HBV (nucleo)capsids are not stiff but rather are highly dynamic entities, as has been recently demonstrated in an impressive all-atom molecular dynamics simulation on the microsecond timescale (19).

THE MODULAR ARCHITECTURE OF THE HEPATITIS B VIRUS ENVELOPE PROTEINS

The envelope proteins L, M, and S, together referred to as hepatitis B surface antigen (HBsAg), are encoded by a single ORF and expressed from alternative in-frame start codons. Accordingly, they share the C-terminal S domain (**Figure 3**). M is extended by the PreS2 domain of 55 aa (20, 21), and L is in addition by the PreS1 of 108 or 119 aa, depending on the genotype (22). All PreS1 coordinates provided in the subsequent sections have been converted to the 108 aa variant of HBV, subtype *ayw*, genotype D (23, 24).

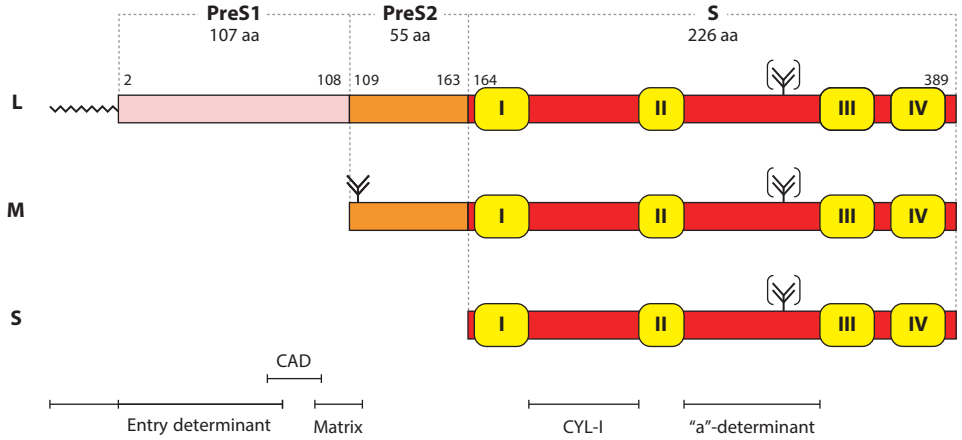

Figure 3

The domain organization of the three HBV envelope proteins. Yellow boxes indicate transmembrane helices. The black zigzag line and arrow nocks indicate N-terminal myristoylation and the *N*-glycosylation, respectively. Abbreviations: aa, amino acid; CAD, cytosolic anchorage determinant; CYL-I, cytosolic loop I; HBV, hepatitis B virus; L, large; M, middle; S, small.

The ORF for the envelope proteins emerged de novo in a nonenveloped progenitor virus ~370 million years ago, concomitant with the appearance of terrestrial vertebrates (3). The primary sequences of S are highly conserved among all hepadnaviruses (3, 25), including the most distantly related group recently found in fishes (3, 26). In contrast, the PreS domains are so diversified that even between more closely related viral species the phylogenetic signal became blurred. This distinction is paralleled on a structural level by S adopting a complex fold, while PreS features intrinsic disorder (27, 28).

The S domain serves as membrane anchor for the envelope proteins. It contains 4 aa stretches forming α-helical transmembrane segments (TM) (**Figure 3**). The amphipathic TM-I (aa15–30 of S) and the hydrophobic TM-II (aa78–104) are separated by the hydrophilic cytosolic loop I (CYL-I). TM-II is followed by a hydrophilic ectodomain, the "a"-determinant, representing the major immunogenic region, against which the host's anti-HBs response is directed. The C-terminal third of S is again largely hydrophobic with TM-III (aa169–199) and TM-IV (aa203–224). Both CYL-I and the "a"-determinant contain several cysteines, the latter involved in disulfide bonding within and between envelope protein homo- and heterodimers, creating an oligomeric network in the viral membrane (29–32).

This basic architecture of S is common to all hepadnaviruses discovered so far, except that the "a"-determinant is unique to the mammalian members of the family and the closely related metahepadnaviruses infecting ray-finned fishes (3). In all other known hepadnaviral species, TM-II and -III are separated by a short loop.

The S domain of all three envelope proteins becomes *N*-glycosylated at Asn-146 in the "a"-determinant in about half of the molecules (33, 34). This leads to the characteristic double band patterns in sodium dodecyl sulfate-polyacrylamide gel electrophoresis of HBV particles under reducing conditions (22, 35). M is constitutively *N*-glycosylated at aa4 of PreS2 (21, 36), unlike L, in which neither this nor sites in the N terminus of PreS1 are naturally utilized.

The L protein undergoes myristoylation at Gly-2 after removal of the start methionine (37). Myristoylation is essential for infectivity (38, 39) but not for viral assembly (40). Myristoylation consensus motifs including a glycine residue at position 2 of L can be identified in most, but not all, hepadnaviruses known (41).

The PreS domains are rich in proline, which is typical for intrinsically disordered proteins (42–44). Notably, disorder is a common feature of viral proteins encoded by overlapping ORFs that emerged de novo by overprinting of a preexisting viral gene in a shifted reading frame (45–49). The S domain with its complex transmembrane topology is seemingly an exception to this rule. PreS1 contains several prestructured motifs (50), i.e., short stretches that in solution underlie an equilibrium between disorder and a transient local fold (reviewed in 51).

PreS1 harbors an array of successive linear modules, which contribute essential functions during viral entry (52–54) and particle morphogenesis (40) (**Figure 3**). The first 77 aa comprise the major determinant of infectivity, mediating entry into the host cell. Mutant scanning analyses revealed that successive deletions of 5 aa in this region abrogated infectivity without affecting virion morphogenesis (55). The core function for viral entry is held by the conserved motif NPLGFFP (aa9–15) acting in concert with the N-terminal myristyl moiety (56, 57). This motif mediates the high-affinity interaction with the uptake and fusion receptor sodium-taurocholate cotransporting polypeptide (NTCP) (58–60). Myristoylated synthetic peptides derived thereof act as potent entry inhibitors currently in clinical evaluation (1, 61–64). The infectivity determinant is followed by the cytosolic anchorage determinant, a binding site for heat shock protein Hsc70 mapped to PreS1 aa70–94 (65–67). Residues 92–113, extending into PreS2, constitute the matrix domain (MD), a key element for nucleocapsid envelopment (68). The remaining 50 residues of PreS2 do

not contain any essential modules (68–70) but fulfill a spacer function and can be largely deleted or entirely replaced by a randomized sequence (71, 72).

Likewise, the M protein, unique to mammalian hepadnaviruses (41), is essential for neither morphogenesis nor infectivity (40), and M-deficient mutants frequently emerge during chronic infection (73–75). The S protein alone is sufficient to drive secretion of 20-nm HBsAg spheres (29, 33, 34, 76–79), and thus heterologously expressed S became the first vaccine worldwide produced via recombinant DNA technology (80). The secretion competence of S is opposed by a secretion inhibitory effect of L (37, 81–85). When L is overly expressed, particle secretion ceases and HBsAg becomes trapped intracellularly at the endoplasmic reticulum (ER). The retention signal has been mapped to the extreme N terminus of PreS1 yet is independent of myristoylation (40, 86). The formation of Dane particles, in contrast to SVP, absolutely depends on the presence of both L and S (40, 87). The opposing effects of both proteins on secretion might be involved in creating local patches with an optimal L:S ratio at the ER membrane to support nucleocapsid envelopment (83).

This complex interplay leads to a differential distribution of the three envelope proteins among the different types of viral particles. Spherical SVP consist almost exclusively of S and M proteins with L accounting for only about 1% of the total HBsAg. The average content of L is increased in filamentous SVP to ∼10% of total HBsAg. The envelopes of Dane particles are highly enriched with L representing one in six (22) or even four (88) molecules.

TOPOLOGY OF THE ENVELOPE PROTEINS

S and M Topology

Early evidence for the tertiary fold and membrane topology came from the observation that secreted SVP were resistant to proteolytic cleavage by trypsin, despite the presence of many potential cleavage sites in the primary sequence (33). The elucidation of the transmembrane topology was first approached experimentally by Eble et al. (89–91) in a series of three consecutive studies. These authors introduced a coupled in vitro translation/translocation system for S in the presence of canine pancreatic microsomes (89). Only in the presence of microsomes did the glycosylated species of S emerge, indicating translocation of the "a"-determinant into the vesicles' lumen. The incomplete resistance of the translation product to proteolytic cleavage demonstrated at the same time that S was not entirely secreted into the vesicles' lumen but retained parts of its polypeptide chain on the extraluminal (cytosolic) side. This seminal work demonstrated that S is an integral transmembrane protein and that membrane insertion and translocation of the "a'"-determinant occur, at least in a significant fraction of the molecules, cotranslationally. Moreover, it revealed that topogenic signals mediating membrane insertion reside internally, in contrast to typical cleaved N-terminal signal peptides. Eble and colleagues came up with a preliminary topological model (model i in **Figure 4*a***) and proposed that S protein subunits aggregate at and bud from intracellular membranes as primary lipoprotein particles after extrusion of host membrane proteins and reorganization of lipids.

Subsequently, Eble et al. (90) provided a detailed genetic mapping of the major topogenic signals in S. They identified a first signal comprising TM-I, which is capable of mediating secretion of adjacent regions across membranes, and the absence of any intrinsic stop transfer signal upstream of TM-II, resulting in an entirely luminal deposition of the respective polypeptides. A distinct second topogenic signal comprising TM-II promoted membrane translocation of adjacent C-terminal sequences but at the same time elicited a stop transfer function creating a type-II-like transmembrane topology. Based on these results, the authors presented a refined topological

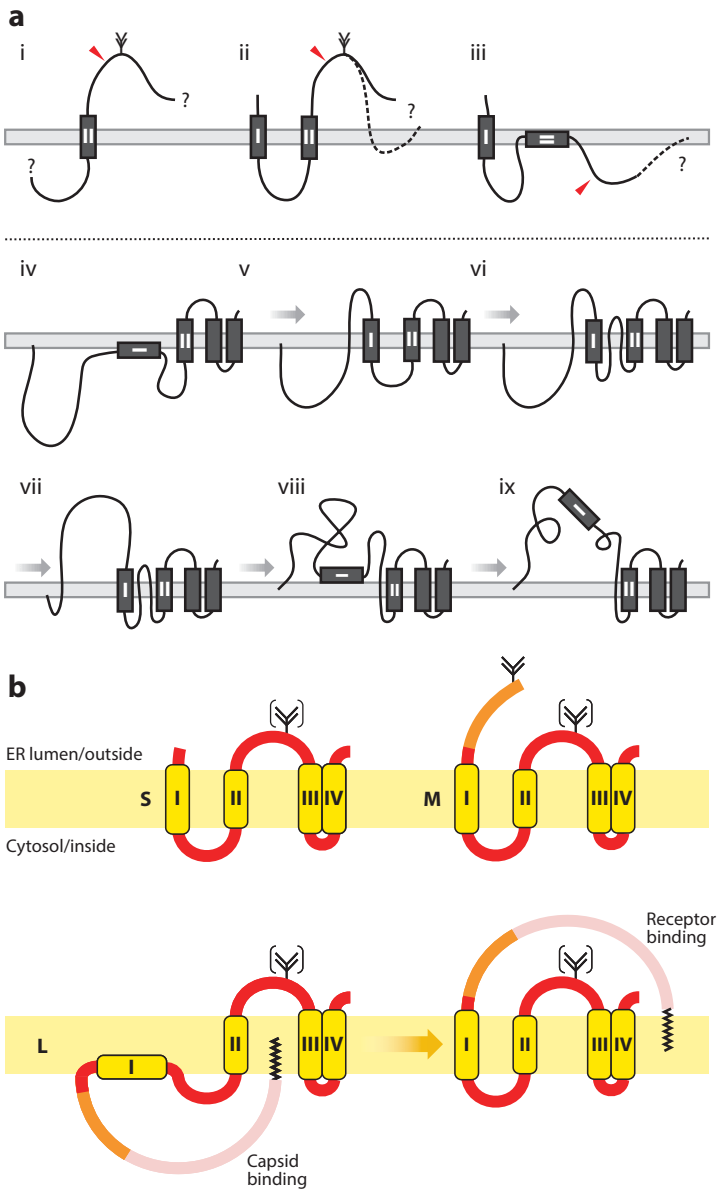

Figure 4

Topology of the envelope proteins. (*a*) Evolution of the models for envelope protein transmembrane topology. (*a*, *i–iii*) HBV S; (*a*, *iv–ix*) DHBV L. The red triangles indicate the marker trypsin cleavage site. The arrow nocks indicate glycosylation at Asn-146. (*b*) Currently accepted standard models of S, M, and L topology. Abbreviations: DHBV, duck hepatitis B virus; ER, endoplasmic reticulum; HBV, hepatitis B virus; L, large; M, middle; S, small.

model of S spanning the membrane bilayer at least twice (**Figure 4*a*, subpanel *ii***). Furthermore, they could show that both signals exploit the cellular translocon machinery at the ER membrane.

The third paper of the Eble et al. series (91) was dedicated to the transmembrane topology of M. The glycosylation and proteolytic fragmentation patterns indicated that the PreS2 region

cotranslationally translocated onto the luminal side, while the S domain of M adopted the same transmembrane topology known from S.

Based on these studies, the currently accepted standard models of the S and M topology have been derived (**Figure 4*b***). Although the exact topology of the hydrophobic C-terminal portion of S, comprising putative TM-III and -IV, still awaits thorough experimentation, the models are supported by bioinformatics approaches to predict protein transmembrane topology, e.g., the MEMSAT3 algorithm (92–94). Nevertheless, these models likely are largely oversimplified. One study revealed strong evidence for a nonuniform topology of S by showing in vitro that the nonglycosylated form, although embedded into microsomal membranes, was fully susceptible to trypsin cleavage within the "a"-determinant (95). Therefore, the authors proposed an alternative model for the nonglycosylated envelope protein species in which TM-II becomes embedded in the plane of the membrane and the "a"-determinant faces the cytosol (**Figure 4*a***, **subpanel *iii***). It is unknown whether these molecules remain fixed in their initial state or adopt the standard topology post-translationally.

L Topology

Early evidence indicated that the PreS region of L is exposed at the viral surface and is highly immunogenic. Antibodies directed against epitopes in PreS1 could efficiently react with HBV particles (22, 96, 97), but recognition was abolished by prior trypsin digestion of the particles (22). Moreover, the N terminus of PreS1 contains a motif responsible for hepatocyte attachment (52), which in turn could be inhibited by antibodies recognizing a short linear epitope close to the N terminus of PreS1 (98). The anti-PreS immune response in patients furthermore correlates with viral clearance and recovery from acute infection (99–102). While these observations argued for an external exposition of PreS, some findings were in conflict. First, L does not become *N*-glycosylated in PreS, despite the presence of consensus sites. Second, the L protein is indispensable for nucleocapsid envelopment and virion formation (87, 103, 104). This puzzling picture was unraveled in three independent studies within a short period of time.

By applying the coupled in vitro translation-translocation, Ostapchuk et al. (105) demonstrated an initial cytoplasmic deposition of the PreS domains of L, contradicting the model ruling at that time. From this, the authors derived their novel topological model of L shown in **Figure 4*b***. These results were independently confirmed and further extended by Bruss et al. (106), who chose a complementary approach by metabolically labeling nascent HBV envelope proteins in cell culture, followed by the determination of the topology in microsomal vesicles. Also in this assay the PreS domains of L were fully degraded by trypsin. Thus, the cotranslational retention of PreS on the cytosolic compartment is a phenomenon also manifest inside an authentic cellular environment. Bruss et al. (106) furthermore provided an analysis of the L topology in secreted viral particles. Proteolytic digests of Dane particles purified from carrier plasma revealed that the PreS domains of only half of the L molecules were susceptible to degradation, while the other half were protected, indicative for being completely hidden within the virions. Overnight incubation at pH 5.5 and 37°C substantially increased the fraction of L with external PreS domains, which implied structural dynamics with post-translational translocation through the viral particle membranes.

In the third independent study discovering the dual L topology, Prange & Streeck (95) for the first time provided kinetic analyses that allowed a direct monitoring of the post-translational, translocon-independent PreS translocation. By performing pulse-chase metabolic labeling of nascent L polypeptides, PreS was found to be entirely cytosolic in the beginning. After a 2-h chase approximately half of the PreS chains had crossed microsomal membranes, and after 4 h PreS was uniformly located on the luminal side.

The deletion of PreS1 aa70–94 supported the emergence of double- and triple-glycosylated forms of L at the ER, indicative of the presence of a motif, termed cytosolic anchorage determinant (CAD), suppressing immediate cotranslational PreS translocation (**Figure 3**). The function of the CAD in cotranslational PreS retention relies on its interaction with the chaperone Hsc70, regulated by several other host factors (65–67, 107).

Interestingly, neither TM-I, nor TM-III and -IV of L are required to facilitate post-translational PreS translocation (108, 109). Rather, the hydrophobic TM-II alone is sufficient to drive the transport of PreS across the membrane (108, 109).

Together, these data unveiled an exceptional case of a protein adopting alternative membrane orientations of a subdomain, which serves distinct functions. Because PreS has to be actively held back on the cytosolic side by Hsc70, the nontranslocated form of L must be metastable with the intrinsic propensity to undergo spontaneous relocation. Although the mechanism remains unknown, it might involve rather forceful events instead of a smooth sliding. The three initial studies left open how PreS translocation and virion formation are temporally related. For instance, Ostapchuk et al. (105, p. 1048) wrote, "during or following budding a dramatic reorganization of either the envelope proteins or the lipid bilayer (or both components) must occur to allow surface display of these sequences." Bruss et al. (106) furthermore provided evidence for dynamics of the topology in Dane particles isolated from chronic carriers. Nevertheless, it soon thereafter became a majority opinion that the dual topology of L is established already at the ER membrane before envelopment of nucleocapsids and that budded virions hence contain a preformed, stable 50:50 distribution of both topological forms in their envelopes. It was not until more than 20 years later that the idea of a topological switch taking place in virions as a distinct maturation step was revived (see the sections titled Cryo–Electron Microscopy Indicates Ultrastructural Dynamics in Virions and a Distinct Maturation Step Renders Dane Particles Infectious).

THE LUCK OF HAVING A DUCK

An even more elaborate view on the ultrastructural dynamics of hepadnaviral envelope protein topogenesis emerged from studying duck hepatitis B virus (DHBV) as a surrogate for HBV (110). DHBV encodes for only two envelope proteins, S and L (PreS+S) (41). The PreS domain of DHBV L contains the major determinants for attachment and entry into the host cell (111–114). That DHBV exhibits a similar dual topology of L was established soon after publication of the pioneer studies for HBV. By use of the cell-free coupled in vitro translation-translocation assay (115) and pulse-chase labeling experiments in DHBV-infected primary duck hepatocytes (PDH) (116), it was demonstrated that PreS was entirely cytosolic immediately after synthesis of L and integration of the S domain into ER membranes, followed by post-translational membrane translocation taking place in a post-ER compartment (**Figure 4*a***, **subpanels *iv*,*vii***). In DHBV particles purified from serum of infected ducks, about 50% of the L molecules were sensitive or resistant to proteolysis, indicating a mixed topology similar to HBV (116). A finer resolution was obtained by Guo & Pugh (115) in showing that virtually all L molecules in DHBV particles display a short polypeptide stretch close to the PreS-S junction on their exterior, although the upstream PreS segment still resided internally in about half of the L molecules (**Figure 4*a***, **subpanel *v***). From this, the authors concluded the existence of a translocation-ready intermediate, in which TM-I had already inserted perpendicularly into the membrane (**Figure 4*a***, **subpanel *v***). Moreover, also the CYL-I of L could be shown to traverse the membrane twice (117), resulting in the exposure of a short epitope at its center on the particle surface (**Figure 4*a***, **subpanel *vi***). In contrast to HBV, the efficient topological reorientation of DHBV L requires the presence of S and a C-terminally

truncated 10-kD derivative thereof, designated S_t, which in concert act as chaperones guiding post-translational PreS translocation (117, 118).

The DHBV model turned out to be indispensable for the detailed characterization of secondary conformational changes in L during entry into the host hepatocytes. Upon treatment of DHBV particles with dithiothreitol (DTT) or low pH, all L in the particle membrane undergo a major structural rearrangement, during which TM-I relocates out of the membrane onto the surface, while the upstream PreS region adopts a trypsin-resistant tertiary fold (119) (**Figure 4*a***, **subpanels *viii*, *ix***). These results confirm the slippery nature of TM-I and the cytosolic loop lacking an intrinsic stop-transfer function (90). DTT treatment left viral particles soluble and virions infective. Low pH treatment, on the contrary, increased the surface hydrophobicity leading to particle aggregation, while infectivity was lost. Therefore, the DTT-induced conformational switch was interpreted to represent a prefusion state in which the amphipathic TM-I helix, although relocated onto the particle surface, was either still oriented with its hydrophobic side facing toward the particle membrane or masked by the PreS fold (**Figure 4*a***, **subpanel *viii***). Acidification was supposed to trigger the release of a metastable spring-loaded conformation, due to which TM-I became fully exposed, thus mimicking the fusion process that—if proceeding abortively in absence of a target membrane—ends up in an irreversible inactivation of viral infectivity (**Figure 4*a***, **subpanel *ix***). If this happens at the right place and time, i.e., after receptor-mediated endocytosis of virions (120, 121) and transport to the late endosomal compartment (pH 5.5), TM-I of the L protein fulfills its essential function as a fusion peptide, resulting in productive infection of PDH (122).

The example of DHBV provides further evidence for the exceptional conformational variability of hepadnaviral L and its dynamics during morphogenesis and entry (step 4 in **Figure 1*b***). The extent to which the data about the secondary changes involved in entry of DHBV also apply to HBV is not yet clear. That a similar secondary PreS folding and relocation of TM-I onto the surface might occur in HBV, too, is supported by the finding that TM-I of L is crucial for infectivity by acting as a fusion peptide (72, 123–126). The interplay between TM-I and the myristoylated N-terminal infectivity determinant in PreS1 during the fusion process still awaits elucidation.

SELECTIVITY OF THE INTERACTIONS BETWEEN ENVELOPE PROTEINS AND NUCLEOCAPSIDS: AN UNRESOLVED ISSUE

In accordance with its highly condensed genome organization, HBV does not encode for a dedicated matrix protein. The nucleocapsid rather interacts directly with the membrane-embedded surface proteins and thus accomplishes envelopment and virion secretion. Determinants for this interaction reside in both PreS and S domains of the envelope proteins. These determinants were identified in mutagenesis studies investigating virion formation in cell culture and in vitro interaction studies between envelope protein–derived peptides and liver-derived HBV nucleocapsids.

A peptide comprising the C-terminal half of the CYL-I (S residues 56–80, see **Figure 3**) was identified as a binding partner in vitro directly by its ability to capture nucleocapsids and indirectly by its inhibitory effect on immune recognition of these particles with anti-HBc (127). A peptide representing the N-terminal part of CYL-I (residues 31–55 of S) failed to bind in these assays yet also contributes to binding, as was shown by Löffler-Mary et al. (128) in cell culture via complementation of envelope protein-deficient HBV genomes *in trans*. This assay allowed the genetic mapping of binding determinants within the envelope proteins by introducing deletions, short replacements, or insertions. Mutations in the N-terminal half of CYL-I, comprising residues 33–59 of the S domain, retained competence to release intact SVP but interfered with nucleocapsid envelopment (**Figure 3**). Importantly, the *trans*-complementation assay established that the

determinant in CYL-I acts in the context of the S protein but not significantly in the context of L, indicating for the first time a differential role for both proteins in envelopment. Löffler-Mary et al. (128) concluded that the binding site is not a continuous linear motif but that it is conformational.

The finding that L and S are absolutely required for virion morphogenesis (40) led to the hypothesis that PreS bears a determinant critical for nucleocapsid envelopment. In a *trans*-complementation assay in cell culture, N-terminal truncations in L up to PreS1 residue 91 were well tolerated, while any further deletion abrogated virion formation (104). The same result was independently obtained investigating the effect of short internal deletions in PreS1 on virion secretion and infectivity (55). Likewise, the fusion of a signal peptide to the N terminus of PreS1 prompting immediate cotranslational translocation abolished nucleocapsid envelopment (129). The determinant required for virion morphogenesis, ultimately termed MD, was mapped to residues 92–113, thus comprising the C-terminal 17 aa of PreS1 and the first 5 aa of PreS2 (68). This result could be confirmed independently by in vitro binding of a synthetic peptide to nucleocapsids (127). Extended mutational profiling of the MD revealed a very high constraint on sequence variability (130). PreS2 downstream of the MD was shown not to contain any functional motifs relevant to virion formation and infectivity (69, 72). Even extended deletions of PreS2 and the adjacent S domain, leaving as few as 26 out of 129 residues between the MD and TM-II, were tolerated with respect to nucleocapsid envelopment (71). These 26 residues were interpreted as the minimal spacer to bridge the distance between the membrane and the MD target sites on the nucleocapsid surface.

The major binding site on nucleocapsids has been mapped by mutational profiling (131–133). Residues essential for envelopment are discontinuously distributed over the primary sequence of the C protein but cluster in the quaternary structure on the surface of the C dimers at a ring-like groove surrounding the spike base and close to the holes in the capsid shell (**Figure 2*b***). The distance of these sites to the spike tips, and thus to the viral membrane, is well compatible with the length of the minimal spacer required between the MD and TM-II (71). Another binding region was assumed on the tips of the spikes because a phage display-selected peptide binding to this region inhibited the binding of capsids to L (134–136). However, attempts to demonstrate a direct interaction between PreS-derived peptides and the spike tips failed (137), and thus it is likely that binding of the phage-selected peptides to the tips created a spatial hindrance preventing the MD from reaching its putative binding site at the spike base. The critical importance of the interaction between the MD and the nucleocapsid has been further elaborated in detail in a recent study by Pastor et al. (138) in which C, L, and S proteins were coexpressed in hepatocytes from separate constructs. In a series of confocal microscopy and coimmunoprecipitation experiments, these authors demonstrated that L serves as a docking platform recruiting both capsids and S protein subunits to the same perinuclear sites, while S alone did not interact strongly enough to yield a similar redirection of capsids.

Envelopment of HBV capsid particles was shown to be a selective process discriminating between different maturation states of the encapsidated viral genome. The observation that mature dsDNA represents the predominant genome species in secreted virions (139, 140) initiated studies in cell culture investigating the prerequisites for nucleocapsids to acquire the competence to become enveloped. HBV nucleocapsids were artificially arrested in different states of genome maturation by introducing missense mutations into P, rendering either the reverse transcriptase or RNase H domain nonfunctional (141). It turned out that nucleocapsids become efficiently enveloped only if they contain more rigid double-stranded forms of the viral genome (authentic relaxed circular DNA or artificial RNA/DNA hybrids), while nucleocapsids containing single-stranded genome intermediates were excluded from this process. To explain this

phenomenon, it was proposed that information about the progress of reverse transcription inside the nucleocapsid was transmitted to the outside by a maturation signal, possibly an alteration of the capsid ultrastructure.

In line with this notion was the discovery of C protein mutant F97L (or I97L, depending on the HBV subtype) displaying an immature secretion phenotype in cell culture (142–145). This mutant, frequently found in chronic patients, is characterized by the preferential envelopment of nucleocapsids containing minus-strand single-stranded DNA (ssDNA) (143). The excess secretion of virions containing ssDNA is even more pronounced in vivo, as was demonstrated recently in a mouse model (146). The mutation at C position 97, directly adjacent to the region mapped to mediate MD binding, could be reverted to a wild-type phenotype by a compensatory mutation in the MD of PreS (A108F). Thus, it was concluded that the 97L mutants lead to a superefficient interaction of immature ssDNA-containing nucleocapsids with the MD domain of L. The high-resolution structure of *E. coli*–derived F97L capsids determined by cryo–electron microscopy (cryo-EM) revealed some subtle changes close to the MD-binding region at the base of the spikes that might be involved in the enhanced capability to interact with PreS (147).

Due to the utilized readout systems, the above studies considered only nucleocapsids with enclosed viral nucleic acid but disregarded capsids devoid of viral genetic material, which can also become enveloped and secreted as virus-like particles (VLP) (148). To account for that, Schormann et al. (149) expressed C and envelope proteins in absence of pgRNA and P and compared the efficiency of empty VLP formation to virion formation from nucleocapsids enclosing pgRNA or mature viral DNA. In accordance with the maturation signal hypothesis, they found a greatly reduced efficiency of envelopment for empty capsids and pgRNA-containing nucleocapsids compared to nucleocapsids harboring mature viral genomes. Moreover, the low envelopment efficiency of empty 97L mutant capsids demonstrated that the immature secretion phenotype strictly depends on the incorporation of a functional replication complex and initiation of reverse transcription. The authors predicted that recombinant *E. coli*–derived 97L capsid particles would not elicit the full-blown manifestation of the proposed maturation signal (149).

However, the maturation signal model was challenged by the observation of an excess of noncanonical, genome-free Dane particles enclosing empty capsids both in vivo and in cell culture (150–153). Envelopment of the genome-free capsids did not require interaction with L protein but rather was mediated by S protein (154). Therefrom, the alternative single-strand blocking model was derived (153) (**Figure 5**), which postulates the presence of (*a*) a secretion signal I responsible for driving envelopment of genome-free capsids, (*b*) a blocking signal dominant over signal I preventing envelopment of nucleocapsids containing single-stranded genome intermediates, and (*c*) a distinct second signal II appearing upon plus-strand DNA synthesis, which in concert with signal I and the removal of the blocking signal promotes the interaction with the MD of L, resulting in the release of complete infectious Dane particles (154).

Of note, the occurrence of aberrant Dane particles with empty capsids in the serum of chronically infected HBV carriers is a phenomenon known since the late 1970s (155–159). These noncanonical virions can be separated from full ones by equilibrium density gradient centrifugation due to their slightly lower buoyant density and are characterized by the lack of an endogenous polymerase activity (156). In transmission electron microscopy, they can be recognized by the penetration of stain into the capsids' interior. Interestingly, empty Dane particles were shown to contain capsids built not from C protein dimers but from a Precore (PreC) protein species (160) (**Figure 2*a***). This finding might be explained by the observation that after proteolytic processing, about 15% of the PreC proteins recycle back into the cytoplasm rather than becoming secreted as mature e-antigen (161–165) (**Figure 2*a***). The reducing conditions in the cytoplasm then trigger a dramatic conformational switch in quaternary structure rendering the reimported PreC dimers

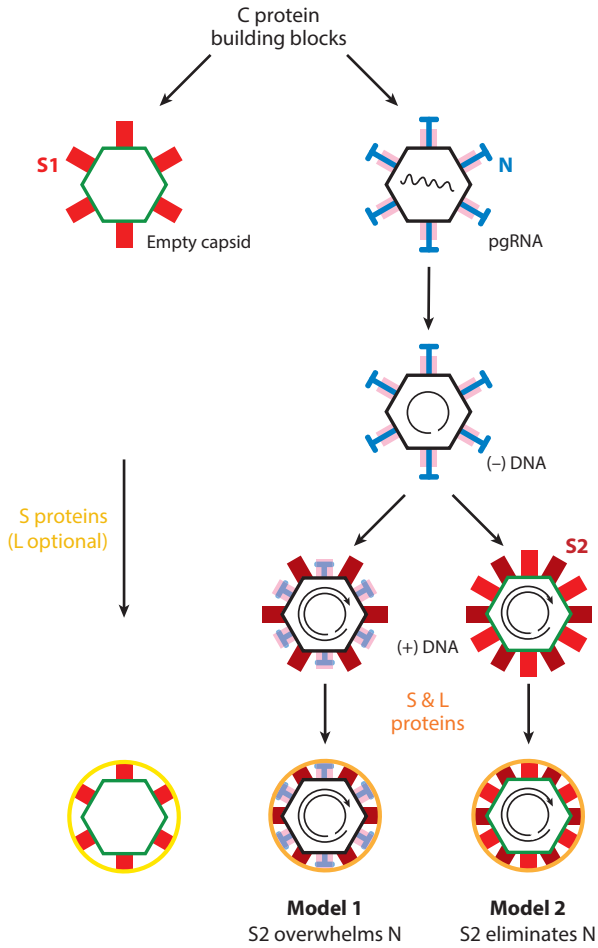

Figure 5

The single-strand blocking model postulates three signals encoded in the capsid, which together regulate envelopment (153, 154). S1, a positive secretion signal, is constitutive in all (nucleo)capsids yet is subordinate to N. The latter is a negative retention signal occurring in immature nucleocapsids containing single-stranded nucleic acids. S2 appears only in mature nucleocapsids and is dominant over N. S1 triggers an interaction with S protein (*yellow*), while S2 mediates binding to the MD domain of L (*orange*). Abbreviations: C, core; L, large; MD, matrix domain; pgRNA, pregenomic RNA; S, small.

competent to coassemble with C protein dimers into mixed heterocapsids devoid of viral replication complexes (164, 166–169).

The fraction of empty Dane particles circulating in the bloodstream is highly variable between chronic patients (and probably also within any individual patient during the course of chronic infection) and correlates inversely with the viral replication activity: The fraction of empty virions is high in low-titer sera, and vice versa (157). One plausible explanation is that Dane particles with empty capsids arise at more constant baseline levels and become the predominant species when the production of infectious virions decreases or even ceases over time, as typically happens in the late phases of chronic HBV infection. Noteworthy, somatic integration of non-canonical, linearized HBV DNA species into the genomes of hepatocytes can be detected

frequently within hours after virus transmission (170). The emergence of such integrations involves the host cellular DNA repair machinery, and they persist in chronically infected patients throughout life due to clonal expansion of the respective cells (171). Currently, it is unknown whether these integrated viral genomes contribute to the excess of noncanonical empty Dane particles late in infection, but it is possible that adjacent enhancer/promoter elements in the flanking host genome sequences drive some expression of capsid-related protein species.

Moreover, a recent study found cellular DNase I to act as a restriction factor of HBV, thus opening the possibility of yet another, quite different mechanism for the emergence of genome-free Dane particles (172). DNase I, whose expression level is heavily upregulated under the hypoxic conditions in cirrhotic liver tissue, can become incorporated with pgRNA and P into assembling nucleocapsids and subsequently digests the viral DNA from inside, resulting in secondarily genome-free virions.

Because so far neither the contribution of PreC-containing heterocapsids nor that of secondary DNA degradation to the formation of empty virions has been sufficiently determined, the discrimination between the maturation signal and the single-strand blocking models is difficult at the current stage (**Figure 5**). In order to elucidate the role of the distinct morphogenetic pathways for viral persistence, we regard it as important to describe the interaction between the different kinds of (nucleo)capsid particles and envelope protein determinants by means of quantitative biochemistry.

CRYO–ELECTRON MICROSCOPY INDICATES ULTRASTRUCTURAL DYNAMICS IN VIRIONS

So far, no high-resolution structures of HBV envelope proteins could be obtained. Nevertheless, a handful of studies based on cryo-EM provided some valuable insight into the three-dimensional (3D) organization of the viral particle envelope and its relation to the nucleocapsid (173–177).

The most recent study found spherical SVP obtained from the serum of a chronic carrier to be highly heterogeneous in size and shape (177). Iterative classification nevertheless allowed selecting two larger populations of particles differing in diameter (29 versus 26 nm), which were subjected to 3D reconstruction. The derived models revealed surface protrusions of an average length of ∼30 Å, locally arranged in a regular pattern. Similar protrusions have been previously described to occur on the particle surface in helical and icosahedral reconstructions, respectively, of serum-derived filamentous SVP (176) and Dane particles (174, 175). Interestingly, a typical bilayer profile of the viral membranes appeared in all three particle types, contradicting earlier biochemical studies on the lipid content of HBsAg particles, which predicted the abrogation of the unit membrane structure due to an extrusion of phospholipids during morphogenesis (76, 178). Structures of higher electron densities traversing the bilayer were attributed to the TM domains of the envelope proteins. The arrangement of the surface protrusions and membrane-traversing densities in reconstructions of the Dane particles' envelope exhibited patterns alternating between local order and disorder, suggesting a loose guidance by the capsid symmetry and a degree of lateral mobility of the envelope protein dimers in the membrane (174, 175).

A striking dimorphism appeared in Dane particle images (175) (**Figure 6*a***). In compact virions, the border between nucleocapsid and envelope could not be recognized. In gapped virions, the envelope was clearly distinguishable from the nucleocapsid by a zone of low electron density. Each of these morphotypes made up ∼45% of the total population, and the remaining ∼10% showed contiguous areas of both sorts. Interestingly, similar morphotypes could be observed in cryo-EM images of woodchuck HBV (see figure 3*b* in Reference 179). Compact particles contained significantly more electron density surrounding the capsid spikes in the interspace between envelope and

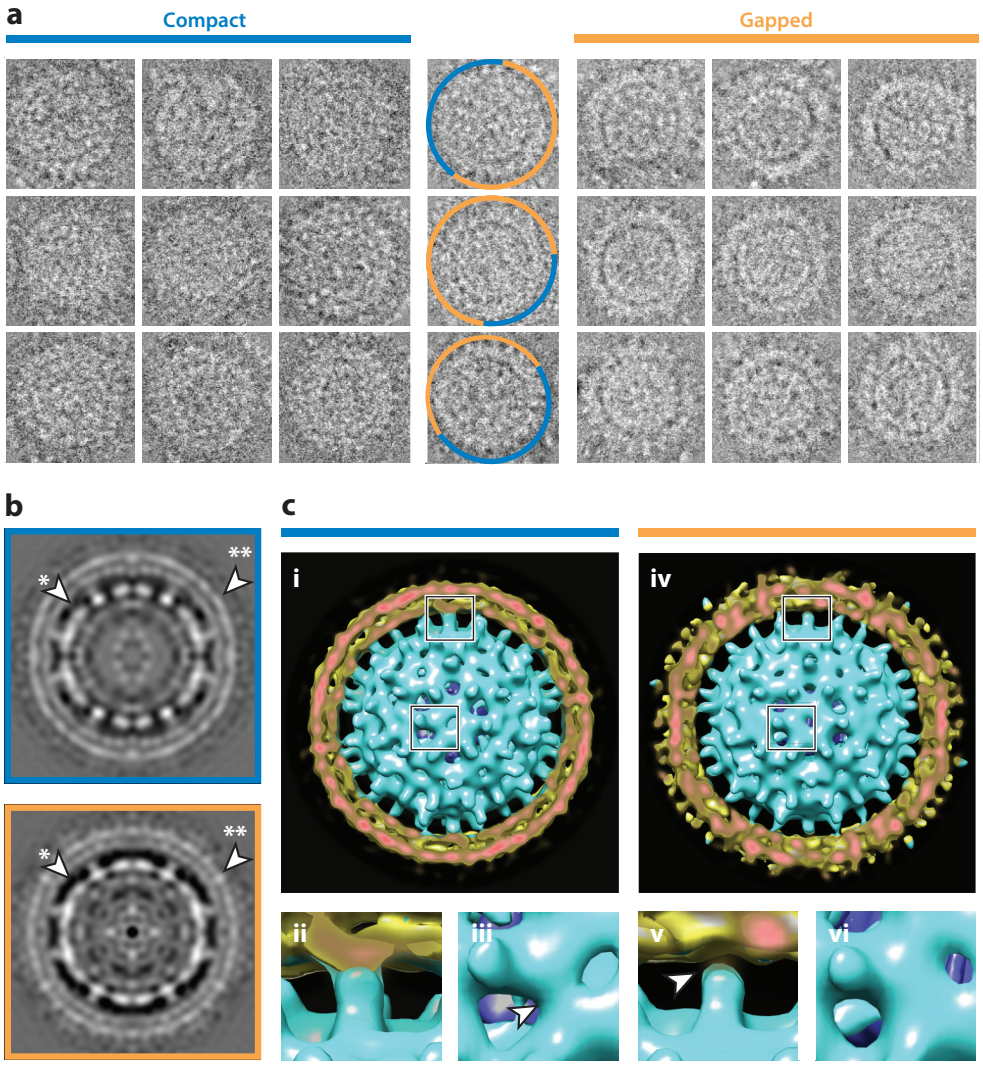

Figure 6

The dual morphology of Dane particles. (*a*) Gallery of compact, gapped, and mixed Dane particles as seen by cryo–electron microscopy. (*b*) Equatorial slices through three-dimensional (3D) reconstructions. Electron density is encoded by gray scale, with white high and black low. A single asterisk indicates where in the capsid-envelope interspace, compact virions contain density absent in the gapped ones. A double asterisk indicates where gapped particles contain more densities traversing the bilayer. (*c*) Refined 3D reconstructions of the most homogenous subpopulations. Subpanels (*i*) and (*iv*): View on the nucleocapsid after cross-section through the envelope. Subpanels (*ii*) and (*v*): Detail view on spike envelope contacts at AB-dimers. Subpanels (*iii*) and (*vi*): Detail view on the interdimer contacts at the pseudo-sixfold axis. The arrow indicates where the B-on-D-contact is weakened in compact particles.

capsid shell (asterisk in **Figure 6*b***). The gapped morphotype, in contrast, displayed more densities traversing the lipid bilayer (double asterisk in **Figure 6*b***) and a higher material content on the outer side of the membrane, while the capsid-envelope interspace apart from the spikes appeared empty (asterisk in **Figure 6*b***). In refined 3D reconstructions of the most homogenous subpopulations, further distinctive features emerged (**Figure 6*c***). In compact virions, the nucleocapsid presented conformational changes, whereas that of gapped ones resembled a reconstruction of

E. coli–derived capsids rendered at similar resolution. At the spikes of the AB capsid dimers, the compact morphotype exhibited intense, bilateral contacts to the envelope. Such contacts were absent in the gapped particles. Moreover, the lipid bilayer profile appeared integer in the compact and rearranged in the gapped morphotype (**Figure 6*c***). The disordered envelope was accompanied by the emergence of additional outer densities.

The visual aspect of the two morphotypes was suggestive of the idea that they differ with regard to the PreS orientation and represent different states of virion maturation. From the distinct structural features, we developed a model of ultrastructural dynamics during Dane particle morphogenesis involving a series of tightly connected, interdependent events (**Figure 1*d***): The peculiar conformation of the nucleocapsids in the compact morphotype represents the proposed maturation signal, or secretion signal II in terms of the single-strand blocking model, that emerges during plus-strand DNA synthesis (step 1 in **Figure 1*d***). The conformational switch might be triggered by pulling forces elicited by P acting on the CTD inside the particles. This assumption is in agreement with the notion that capsids containing dsDNA are in a spring-loaded state (18). The switched conformation has increased affinity for the MD of PreS, resulting in envelopment and secretion of compact Dane particles with intense capsid-envelope contacts (step 2 in **Figure 1*d***). The morphotype of these particles is caused by untranslocated PreS domains in the interspace between the membrane bilayer and the capsid shell. Both the switched capsid conformation and L with untranslocated, internal PreS are metastable structures that keep each other locked in their current state for a certain period of time. Once the capsid reverts to the relaxed state, the interactions between C and PreS subunits are lost again. After detachment from the nucleocapsid, PreS is free to translocate across the viral membrane and becomes exposed on the particle surface. This ultimately results in fully infection-competent Dane particles of the gapped morphotype (step 3 in **Figure 1*d***). Both the transition in the capsid scaffold and PreS translocation might occur spontaneously at one position in the icosahedral lattice. The released energy, in turn, might deliver the activation energy necessary to promote a cascade of similar events at neighboring positions, leading to a rapid and cooperative progression of the conversion throughout the entire particle like a domino effect. This maturation process is a prerequisite to render the particles competent for binding to receptors mediating attachment and uptake into hepatocytes. The subsequent intracellular virus-host membrane fusion is assumed to involve an induced spring-loaded secondary fold of PreS/S such as in DHBV (step 4 in **Figure 1*d***) (119, 122–126).

A DISTINCT MATURATION STEP RENDERS DANE PARTICLES INFECTIOUS

In a follow-up study, we provided evidence for the later steps in our model related to virion maturation (88). We took advantage of the finding that attachment of HBV particles to the cell surface requires the PreS1-dependent interaction with heparan sulfate proteoglycans (HSPGs) as primary receptors (180, 181). Hence, we used affinity chromatography to separate virions with respect to their ability to bind to heparin and demonstrated the existence of two distinct populations: Nonbinders without affinity to heparin had PreS entirely hidden in the particle interior and were noninfectious, while binders exposed PreS on their surface, conferring full infectiousness. Notably, we showed that all Dane particles are released from hepatocytes in the form of nonbinders and subsequently turn into heparin binders in a slow exponential process with a half-time of ~5 h. Furthermore, we revealed that this distinct maturation step provides an efficient mechanism preventing particle loss due to nonproductive HSPG binding in the capillary bed of extrahepatic tissues. Indeed, when administered intravenously at low dose, nonbinders were superior to binders in establishing persistent infections in a human liver chimeric mouse model, explaining the extraordinary transmission efficiency of HBV.

CLOSING COMMENTS

The Dane particle is a highly dynamic entity, and its molecular components rearrange repeatedly during assembly, maturation, and host entry, reflected in morphological changes on an ultrastructural level. The scaffold of this particle is made up of envelope and capsid proteins, each occurring in multiple isoforms and conformational states. Their highly specific interaction accomplishes the envelopment of the emerging nucleocapsid, and, conversely, envelope release prepares viral entry into the host cell. In the past decades, the molecular determinants for envelopment and the architecture of the envelope proteins have been elucidated in vivo and in vitro by extensive molecular biology approaches. Meanwhile, the structures of these integral membrane proteins in the context of Dane particles and SVP remain unknown. Another long-standing research question is the molecular basis of the elusive maturation or blocking signals encoded in the capsid protein conformation or ultrastructure. These signals could be metastable and short-lived because their secondary abrogation might be prerequisite to release nucleocapsids into the cytoplasm during entry into the next host cell. As this signal balances envelopment against nuclear import of nucleocapsids, and thus the production of new virions against maintenance of the viral DNA pool, it has major implications for viral persistence. Hence, these research interests are not entirely academic in nature but carry potential for therapeutic intervention against HBV for which thus far a cure is not available.

DISCLOSURE STATEMENT

The authors are not aware of any affiliations, memberships, funding, or financial holdings that might be perceived as affecting the objectivity of this review.

ACKNOWLEDGMENTS

Work by R.B. is supported by the Deutsche Forschungsgemeinschaft (DFG, German Research Foundation), Projektnummer 272983813, TRR 179. S.S. and A.S. acknowledge seed funds provided by TRR179. A.K.S. acknowledges funding from the DFG, German Research Foundation, project SCHU 3265/1-1.

LITERATURE CITED

1. Bartenschlager R, Urban S, Protzer U. 2019. Towards curative therapy of chronic viral hepatitis. *Z. Gastroenterol.* 57(1):61–73
2. WHO (World Health Organ.). 2019. Hepatitis B: key facts. *World Health Organization*. **http://www.who.int/mediacentre/factsheets/fs204/en/**
3. Lauber C, Seitz S, Mattei S, Suh A, Beck J, et al. 2017. Deciphering the origin and evolution of hepatitis B viruses by means of a family of non-enveloped fish viruses. *Cell Host Microbe* 22(3):387–99
4. Gilbert C, Feschotte C. 2010. Genomic fossils calibrate the long-term evolution of hepadnaviruses. *PLOS Biol.* 8(9):e1000495
5. Suh A, Weber CC, Kehlmaier C, Braun EL, Green RE, et al. 2014. Early Mesozoic coexistence of amniotes and Hepadnaviridae. *PLOS Genet.* 10(12):e1004559
6. Dane DS, Cameron CH, Briggs M. 1970. Virus-like particles in serum of patients with Australia-antigen-associated hepatitis. *Lancet* 1(7649):695–98
7. Seeger C, Mason WS. 2000. Hepatitis B virus biology. *Microbiol. Mol. Biol. Rev.* 64(1):51–68
8. Nassal M. 2008. Hepatitis B viruses: reverse transcription a different way. *Virus Res.* 134(1–2):235–49
9. Watanabe T, Sorensen EM, Naito A, Schott M, Kim S, Ahlquist P. 2007. Involvement of host cellular multivesicular body functions in hepatitis B virus budding. *PNAS* 104(24):10205–10

10. Wynne SA, Crowther RA, Leslie AG. 1999. The crystal structure of the human hepatitis B virus capsid. *Mol. Cell* 3(6):771–80
11. Böttcher B, Wynne SA, Crowther RA. 1997. Determination of the fold of the core protein of hepatitis B virus by electron cryomicroscopy. *Nature* 386(6620):88–91
12. Conway JF, Cheng N, Zlotnick A, Wingfield PT, Stahl SJ, Steven AC. 1997. Visualization of a 4-helix bundle in the hepatitis B virus capsid by cryo-electron microscopy. *Nature* 386(6620):91–94
13. Yu X, Jin L, Jih J, Shih C, Zhou ZH. 2013. 3.5A cryoEM structure of hepatitis B virus core assembled from full-length core protein. *PLOS ONE* 8(9):e69729
14. Patel N, White SJ, Thompson RF, Bingham R, Weiss EU, et al. 2017. HBV RNA pre-genome encodes specific motifs that mediate interactions with the viral core protein that promote nucleocapsid assembly. *Nat. Microbiol.* 2:17098
15. Caspar DL, Klug A. 1962. Physical principles in the construction of regular viruses. *Cold Spring Harb. Symp. Quant. Biol.* 27:1–24
16. Ceres P, Zlotnick A. 2002. Weak protein–protein interactions are sufficient to drive assembly of hepatitis B virus capsids. *Biochemistry* 41(39):11525–31
17. Wang JC, Nickens DG, Lentz TB, Loeb DD, Zlotnick A. 2014. Encapsidated hepatitis B virus reverse transcriptase is poised on an ordered RNA lattice. *PNAS* 111(31):11329–34
18. Dhason MS, Wang JC, Hagan MF, Zlotnick A. 2012. Differential assembly of hepatitis B virus core protein on single- and double-stranded nucleic acid suggest the dsDNA-filled core is spring-loaded. *Virology* 430(1):20–29
19. Hadden JA, Perilla JR, Schlicksup CJ, Venkatakrishnan B, Zlotnick A, Schulten K. 2018. All-atom molecular dynamics of the HBV capsid reveals insights into biological function and cryo-EM resolution limits. *eLife* 7:e32478
20. Machida A, Kishimoto S, Ohnuma H, Baba K, Ito Y, et al. 1984. A polypeptide containing 55 amino acid residues coded by the pre-S region of hepatitis B virus deoxyribonucleic acid bears the receptor for polymerized human as well as chimpanzee albumins. *Gastroenterology* 86(5 Part 1):910–18
21. Stibbe W, Gerlich WH. 1983. Structural relationships between minor and major proteins of hepatitis B surface antigen. *J. Virol.* 46(2):626–28
22. Heermann KH, Goldmann U, Schwartz W, Seyffarth T, Baumgarten H, Gerlich WH. 1984. Large surface proteins of hepatitis B virus containing the pre-*s* sequence. *J. Virol.* 52(2):396–402
23. Pasek M, Goto T, Gilbert W, Zink B, Schaller H, et al. 1979. Hepatitis B virus genes and their expression in *E. coli*. *Nature* 282(5739):575–79
24. Galibert F, Mandart E, Fitoussi F, Tiollais P, Charnay P. 1979. Nucleotide sequence of the hepatitis B virus genome (subtype ayw) cloned in *E. coli*. *Nature* 281(5733):646–50
25. Mandart E, Kay A, Galibert F. 1984. Nucleotide sequence of a cloned duck hepatitis B virus genome: comparison with woodchuck and human hepatitis B virus sequences. *J. Virol.* 49(3):782–92
26. Hahn CM, Iwanowicz LR, Cornman RS, Conway CM, Winton JR, Blazer VS. 2015. Characterization of a novel hepadnavirus in the white sucker (*Catostomus commersonii*) from the Great Lakes region of the United States. *J. Virol.* 89(23):11801–11
27. Lee MK, Kim KL, Hahm KS, Yang KH. 1994. Structure-antigenicity relationship of peptides from the pre-S2 region of the hepatitis B virus surface antigen. *Biochem. Mol. Biol. Int.* 34(1):159–68
28. Maeng CY, Oh MS, Park IH, Hong HJ. 2001. Purification and structural analysis of the hepatitis B virus preS1 expressed from *Escherichia coli*. *Biochem. Biophys. Res. Commun.* 282(3):787–92
29. Huovila AP, Eder AM, Fuller SD. 1992. Hepatitis B surface antigen assembles in a post-ER, pre-Golgi compartment. *J. Cell Biol.* 118(6):1305–20
30. Mangold CM, Streeck RE. 1993. Mutational analysis of the cysteine residues in the hepatitis B virus small envelope protein. *J. Virol.* 67(8):4588–97
31. Wunderlich G, Bruss V. 1996. Characterization of early hepatitis B virus surface protein oligomers. *Arch. Virol.* 141(7):1191–205
32. Suffner S, Gerstenberg N, Patra M, Ruibal P, Orabi A, et al. 2018. Domains of the hepatitis B virus small surface protein S mediating oligomerization. *J. Virol.* 92(11):e02232-17

33. Peterson DL. 1981. Isolation and characterization of the major protein and glycoprotein of hepatitis B surface antigen. *J. Biol. Chem.* 256(13):6975–83
34. Peterson DL, Nath N, Gavilanes F. 1982. Structure of hepatitis B surface antigen. Correlation of subtype with amino acid sequence and location of the carbohydrate moiety. *J. Biol. Chem.* 257(17):10414–20
35. Peterson DL, Roberts IM, Vyas GN. 1977. Partial amino acid sequence of two major component polypeptides of hepatitis B surface antigen. *PNAS* 74(4):1530–34
36. Stibbe W, Gerlich WH. 1983. Characterization of pre-s gene products in hepatitis B surface antigen. *Dev. Biol. Stand.* 54:33–43
37. Persing DH, Varmus HE, Ganem D. 1987. The preS1 protein of hepatitis B virus is acylated at its amino terminus with myristic acid. *J. Virol.* 61(5):1672–77
38. Gripon P, Le Seyec J, Rumin S, Guguen-Guillouzo C. 1995. Myristylation of the hepatitis B virus large surface protein is essential for viral infectivity. *Virology* 213(2):292–99
39. Bruss V, Hagelstein J, Gerhardt E, Galle PR. 1996. Myristylation of the large surface protein is required for hepatitis B virus *in vitro* infectivity. *Virology* 218(2):396–99
40. Bruss V, Ganem D. 1991. The role of envelope proteins in hepatitis B virus assembly. *PNAS* 88(3):1059–63
41. Wang Q, Qin Y, Zhang J, Jia L, Fu S, et al. 2020. Tracing the evolutionary history of hepadnaviruses in terms of e antigen and middle envelope protein expression or processing. *Virus Res.* 276:197825
42. Williamson MP. 1994. The structure and function of proline-rich regions in proteins. *Biochem. J.* 297(2):249–60
43. Tompa P. 2003. Intrinsically unstructured proteins evolve by repeat expansion. *Bioessays* 25(9):847–55
44. Theillet FX, Kalmar L, Tompa P, Han KH, Selenko P, et al. 2013. The alphabet of intrinsic disorder: I. Act like a Pro: on the abundance and roles of proline residues in intrinsically disordered proteins. *Intrinsically Disord. Proteins* 1(1):e24360
45. Gitlin L, Hagai T, LaBarbera A, Solovey M, Andino R. 2014. Rapid evolution of virus sequences in intrinsically disordered protein regions. *PLOS Pathog.* 10(12):e1004529
46. Pavesi A, Magiorkinis G, Karlin DG. 2013. Viral proteins originated de novo by overprinting can be identified by codon usage: application to the "gene nursery" of Deltaretroviruses. *PLOS Comput. Biol.* 9(8):e1003162
47. Rancurel C, Khosravi M, Dunker AK, Romero PR, Karlin D. 2009. Overlapping genes produce proteins with unusual sequence properties and offer insight into de novo protein creation. *J. Virol.* 83(20):10719–36
48. Sabath N, Wagner A, Karlin D. 2012. Evolution of viral proteins originated de novo by overprinting. *Mol. Biol. Evol.* 29(12):3767–80
49. Xue B, Blocquel D, Habchi J, Uversky AV, Kurgan L, et al. 2014. Structural disorder in viral proteins. *Chem. Rev.* 114(13):6880–911
50. Chi SW, Kim DH, Lee SH, Chang I, Han KH. 2007. Pre-structured motifs in the natively unstructured preS1 surface antigen of hepatitis B virus. *Protein Sci.* 16(10):2108–17
51. Lee SH, Kim DH, Han JJ, Cha EJ, Lim JE, et al. 2012. Understanding pre-structured motifs (PreSMos) in intrinsically unfolded proteins. *Curr. Protein Pept. Sci.* 13(1):34–54
52. Neurath AR, Kent SB, Strick N, Parker K. 1986. Identification and chemical synthesis of a host cell receptor binding site on hepatitis B virus. *Cell* 46(3):429–36
53. Neurath AR, Seto B, Strick N. 1989. Antibodies to synthetic peptides from the preS1 region of the hepatitis B virus (HBV) envelope (env) protein are virus-neutralizing and protective. *Vaccine* 7(3):234–36
54. Pontisso P, Ruvoletto MG, Gerlich WH, Heermann KH, Bardini R, Alberti A. 1989. Identification of an attachment site for human liver plasma membranes on hepatitis B virus particles. *Virology* 173(2):522–30
55. Le Seyec J, Chouteau P, Cannie I, Guguen-Guillouzo C, Gripon P. 1999. Infection process of the hepatitis B virus depends on the presence of a defined sequence in the pre-S1 domain. *J. Virol.* 73(3):2052–57
56. Urban S, Bartenschlager R, Kubitz R, Zoulim F. 2014. Strategies to inhibit entry of HBV and HDV into hepatocytes. *Gastroenterology* 147(1):48–64

57. Tu T, Urban S. 2018. Virus entry and its inhibition to prevent and treat hepatitis B and hepatitis D virus infections. *Curr. Opin. Virol.* 30:68–79
58. Yan H, Zhong G, Xu G, He W, Jing Z, et al. 2012. Sodium taurocholate cotransporting polypeptide is a functional receptor for human hepatitis B and D virus. *eLife* 3:e00049
59. Ni Y, Lempp FA, Mehrle S, Nkongolo S, Kaufman C, et al. 2014. Hepatitis B and D viruses exploit sodium taurocholate co-transporting polypeptide for species-specific entry into hepatocytes. *Gastroenterology* 146(4):1070–83
60. Li W, Urban S. 2016. Entry of hepatitis B and hepatitis D virus into hepatocytes: basic insights and clinical implications. *J. Hepatol.* 64(1 Suppl.):S32–40
61. Gripon P, Cannie I, Urban S. 2005. Efficient inhibition of hepatitis B virus infection by acylated peptides derived from the large viral surface protein. *J. Virol.* 79(3):1613–22
62. Petersen J, Dandri M, Mier W, Lutgehetmann M, Volz T, et al. 2008. Prevention of hepatitis B virus infection *in vivo* by entry inhibitors derived from the large envelope protein. *Nat. Biotechnol.* 26(3):335–41
63. Schulze A, Schieck A, Ni Y, Mier W, Urban S. 2010. Fine mapping of pre-S sequence requirements for hepatitis B virus large envelope protein-mediated receptor interaction. *J. Virol.* 84(4):1989–2000
64. Bogomolov P, Alexandrov A, Voronkova N, Macievich M, Kokina K, et al. 2016. Treatment of chronic hepatitis D with the entry inhibitor myrcludex B: first results of a phase Ib/IIa study. *J. Hepatol.* 65(3):490–98
65. Löffler-Mary H, Werr M, Prange R. 1997. Sequence-specific repression of cotranslational translocation of the hepatitis B virus envelope proteins coincides with binding of heat shock protein Hsc70. *Virology* 235(1):144–52
66. Prange R, Werr M, Löffler-Mary H. 1999. Chaperones involved in hepatitis B virus morphogenesis. *Biol. Chem.* 380(3):305–14
67. Lambert C, Prange R. 2003. Chaperone action in the posttranslational topological reorientation of the hepatitis B virus large envelope protein: implications for translocational regulation. *PNAS* 100(9):5199–204
68. Bruss V. 1997. A short linear sequence in the pre-S domain of the large hepatitis B virus envelope protein required for virion formation. *J. Virol.* 71(12):9350–57
69. Le Seyec J, Chouteau P, Cannie I, Guguen-Guillouzo C, Gripon P. 1998. Role of the pre-S2 domain of the large envelope protein in hepatitis B virus assembly and infectivity. *J. Virol.* 72(7):5573–78
70. Lepere C, Regeard M, Le Seyec J, Gripon P. 2007. The translocation motif of hepatitis B virus envelope proteins is dispensable for infectivity. *J. Virol.* 81(14):7816–18
71. Kluge B, Schlager M, Pairan A, Bruss V. 2005. Determination of the minimal distance between the matrix and transmembrane domains of the large hepatitis B virus envelope protein. *J. Virol.* 79(12):7918–21
72. Ni Y, Sonnabend J, Seitz S, Urban S. 2010. The pre-s2 domain of the hepatitis B virus is dispensable for infectivity but serves a spacer function for L-protein-connected virus assembly. *J. Virol.* 84(8):3879–88
73. Fernholz D, Stemler M, Brunetto M, Bonino F, Will H. 1991. Replicating and virion secreting hepatitis B mutant virus unable to produce preS2 protein. *J. Hepatol.* 13(Suppl. 4):S102–S104
74. Santantonio T, Jung MC, Schneider R, Fernholz D, Milella M, et al. 1992. Hepatitis B virus genomes that cannot synthesize pre-S2 proteins occur frequently and as dominant virus populations in chronic carriers in Italy. *Virology* 188(2):948–52
75. Fernholz D, Galle PR, Stemler M, Brunetto M, Bonino F, Will H. 1993. Infectious hepatitis B virus variant defective in pre-S2 protein expression in a chronic carrier. *Virology* 194(1):137–48
76. Gavilanes F, Gonzalez-Ros JM, Peterson DL. 1982. Structure of hepatitis B surface antigen. Characterization of the lipid components and their association with the viral proteins. *J. Biol. Chem.* 257(13):7770–77
77. Liu CC, Yansura D, Levinson AD. 1982. Direct expression of hepatitis B surface antigen in monkey cells from an SV40 vector. *DNA* 1(3):213–21
78. Peterson DL. 1987. The structure of hepatitis B surface antigen and its antigenic sites. *Bioessays* 6(6):258–62
79. Simon K, Lingappa VR, Ganem D. 1988. Secreted hepatitis B surface antigen polypeptides are derived from a transmembrane precursor. *J. Cell Biol.* 107(6 Part 1):2163–68

80. Huzair F, Sturdy S. 2017. Biotechnology and the transformation of vaccine innovation: the case of the hepatitis B vaccines 1968–2000. *Stud. Hist. Philos. Biol. Biomed. Sci.* 64:11–21
81. Cheng KC, Smith GL, Moss B. 1986. Hepatitis B virus large surface protein is not secreted but is immunogenic when selectively expressed by recombinant vaccinia virus. *J. Virol.* 60(2):337–44
82. Chisari FV, Filippi P, McLachlan A, Milich DR, Riggs M, et al. 1986. Expression of hepatitis B virus large envelope polypeptide inhibits hepatitis B surface antigen secretion in transgenic mice. *J. Virol.* 60(3):880–87
83. Persing DH, Varmus HE, Ganem D. 1986. Inhibition of secretion of hepatitis B surface antigen by a related presurface polypeptide. *Science* 234(4782):1388–91
84. Standring DN, Ou JH, Rutter WJ. 1986. Assembly of viral particles in *Xenopus* oocytes: pre-surface-antigens regulate secretion of the hepatitis B viral surface envelope particle. *PNAS* 83(24):9338–42
85. Ou JH, Rutter WJ. 1987. Regulation of secretion of the hepatitis B virus major surface antigen by the preS-1 protein. *J. Virol.* 61(3):782–86
86. Kuroki K, Russnak R, Ganem D. 1989. Novel N-terminal amino acid sequence required for retention of a hepatitis B virus glycoprotein in the endoplasmic reticulum. *Mol. Cell Biol.* 9(10):4459–66
87. Ueda K, Tsurimoto T, Matsubara K. 1991. Three envelope proteins of hepatitis B virus: large S, middle S, and major S proteins needed for the formation of Dane particles. *J. Virol.* 65(7):3521–29
88. Seitz S, Iancu C, Volz T, Mier W, Dandri M, et al. 2016. A slow maturation process renders hepatitis B virus infectious. *Cell Host Microbe* 20(1):25–35
89. Eble BE, Lingappa VR, Ganem D. 1986. Hepatitis B surface antigen: an unusual secreted protein initially synthesized as a transmembrane polypeptide. *Mol. Cell Biol.* 6(5):1454–63
90. Eble BE, Macrae DR, Lingappa VR, Ganem D. 1987. Multiple topogenic sequences determine the transmembrane orientation of the hepatitis B surface antigen. *Mol. Cell Biol.* 7(10):3591–601
91. Eble BE, Lingappa VR, Ganem D. 1990. The N-terminal (pre-S2) domain of a hepatitis B virus surface glycoprotein is translocated across membranes by downstream signal sequences. *J. Virol.* 64(3):1414–19
92. Jones DT. 2007. Improving the accuracy of transmembrane protein topology prediction using evolutionary information. *Bioinformatics* 23(5):538–44
93. Reddy A, Cho J, Ling S, Reddy V, Shlykov M, Saier MH. 2014. Reliability of nine programs of topological predictions and their application to integral membrane channel and carrier proteins. *J. Mol. Microbiol. Biotechnol.* 24(3):161–90
94. Reeb J, Kloppmann E, Bernhofer M, Rost B. 2015. Evaluation of transmembrane helix predictions in 2014. *Proteins* 83(3):473–84
95. Prange R, Streeck RE. 1995. Novel transmembrane topology of the hepatitis B virus envelope proteins. *EMBO J.* 14(2):247–56
96. Kuroki K, Floreani M, Mimms LT, Ganem D. 1990. Epitope mapping of the PreS1 domain of the hepatitis B virus large surface protein. *Virology* 176(2):620–24
97. Mimms LT, Floreani M, Tyner J, Whitters E, Rosenlof R, et al. 1990. Discrimination of hepatitis B virus (HBV) subtypes using monoclonal antibodies to the PreS1 and PreS2 domains of the viral envelope. *Virology* 176(2):604–19
98. Sominskaya I, Pushko P, Dreilina D, Kozlovskaya T, Pumpen P. 1992. Determination of the minimal length of preS1 epitope recognized by a monoclonal antibody which inhibits attachment of hepatitis B virus to hepatocytes. *Med. Microbiol. Immunol.* 181(4):215–26
99. Budkowska A, Dubreuil P, Capel F, Pillot J. 1986. Hepatitis B virus pre-S gene-encoded antigenic specificity and anti-pre-S antibody: relationship between anti-pre-S response and recovery. *Hepatology* 6(3):360–68
100. Budkowska A, Dubreuil P, Maillard P, Poynard T, Pillot J. 1990. A biphasic pattern of anti-pre-S responses in acute hepatitis B virus infection. *Hepatology* 12(6):1271–77
101. Budkowska A, Dubreuil P, Poynard T, Marcellin P, Loriot MA, et al. 1992. Anti-pre-S responses and viral clearance in chronic hepatitis B virus infection. *Hepatology* 15(1):26–31
102. Deepen R, Heermann KH, Uy A, Thomssen R, Gerlich WH. 1990. Assay of preS epitopes and preS1 antibody in hepatitis B virus carriers and immune persons. *Med. Microbiol. Immunol.* 179(1):49–60

103. Bruss V, Ganem D. 1991. Mutational analysis of hepatitis B surface antigen particle assembly and secretion. *J. Virol.* 65(7):3813–20
104. Bruss V, Thomssen R. 1994. Mapping a region of the large envelope protein required for hepatitis B virion maturation. *J. Virol.* 68(3):1643–50
105. Ostapchuk P, Hearing P, Ganem D. 1994. A dramatic shift in the transmembrane topology of a viral envelope glycoprotein accompanies hepatitis B viral morphogenesis. *EMBO J.* 13(5):1048–57
106. Bruss V, Lu X, Thomssen R, Gerlich WH. 1994. Post-translational alterations in transmembrane topology of the hepatitis B virus large envelope protein. *EMBO J.* 13(10):2273–79
107. Prange R. 2012. Host factors involved in hepatitis B virus maturation, assembly, and egress. *Med. Microbiol. Immunol.* 201(4):449–61
108. Lambert C, Prange R. 2001. Dual topology of the hepatitis B virus large envelope protein: determinants influencing post-translational pre-S translocation. *J. Biol. Chem.* 276(25):22265–72
109. Lambert C, Mann S, Prange R. 2004. Assessment of determinants affecting the dual topology of hepadnaviral large envelope proteins. *J. Gen. Virol.* 85(Part 5):1221–25
110. Schultz U, Grgacic E, Nassal M. 2004. Duck hepatitis B virus: an invaluable model system for HBV infection. *Adv. Virus Res.* 63:1–70
111. Klingmuller U, Schaller H. 1993. Hepadnavirus infection requires interaction between the viral pre-S domain and a specific hepatocellular receptor. *J. Virol.* 67(12):7414–22
112. Yuasa S, Cheung RC, Pham Q, Robinson WS, Marion PL. 1991. Peptide mapping of neutralizing and nonneutralizing epitopes of duck hepatitis B virus pre-S polypeptide. *Virology* 181(1):14–21
113. Urban S, Breiner KM, Fehler F, Klingmuller U, Schaller H. 1998. Avian hepatitis B virus infection is initiated by the interaction of a distinct pre-S subdomain with the cellular receptor gp180. *J. Virol.* 72(10):8089–97
114. Glebe D, Urban S. 2007. Viral and cellular determinants involved in hepadnaviral entry. *World J. Gastroenterol.* 13(1):22–38
115. Guo JT, Pugh JC. 1997. Topology of the large envelope protein of duck hepatitis B virus suggests a mechanism for membrane translocation during particle morphogenesis. *J. Virol.* 71(2):1107–14
116. Swameye I, Schaller H. 1997. Dual topology of the large envelope protein of duck hepatitis B virus: determinants preventing pre-S translocation and glycosylation. *J. Virol.* 71(12):9434–41
117. Grgacic EV, Kuhn C, Schaller H. 2000. Hepadnavirus envelope topology: insertion of a loop region in the membrane and role of S in L protein translocation. *J. Virol.* 74(5):2455–58
118. Grgacic EV, Anderson DA. 2005. St, a truncated envelope protein derived from the S protein of duck hepatitis B virus, acts as a chaperone for the folding of the large envelope protein. *J. Virol.* 79(9):5346–52
119. Grgacic EV, Schaller H. 2000. A metastable form of the large envelope protein of duck hepatitis B virus: low-pH release results in a transition to a hydrophobic, potentially fusogenic conformation. *J. Virol.* 74(11):5116–22
120. Breiner KM, Urban S, Schaller H. 1998. Carboxypeptidase D (gp180), a Golgi-resident protein, functions in the attachment and entry of avian hepatitis B viruses. *J. Virol.* 72(10):8098–104
121. Breiner KM, Schaller H. 2000. Cellular receptor traffic is essential for productive duck hepatitis B virus infection. *J. Virol.* 74(5):2203–9
122. Chojnacki J, Anderson DA, Grgacic EV. 2005. A hydrophobic domain in the large envelope protein is essential for fusion of duck hepatitis B virus at the late endosome. *J. Virol.* 79(23):14945–55
123. Lepere-Douard C, Trotard M, Le Seyec J, Gripon P. 2009. The first transmembrane domain of the hepatitis B virus large envelope protein is crucial for infectivity. *J. Virol.* 83(22):11819–29
124. Lu X, Block TM, Gerlich WH. 1996. Protease-induced infectivity of hepatitis B virus for a human hepatoblastoma cell line. *J. Virol.* 70(4):2277–85
125. Rodriguez-Crespo I, Nunez E, Gomez-Gutierrez J, Yelamos B, Albar JP, et al. 1995. Phospholipid interactions of the putative fusion peptide of hepatitis B virus surface antigen S protein. *J. Gen. Virol.* 76(2):301–8
126. Rodriguez-Crespo I, Nunez E, Yelamos B, Gomez-Gutierrez J, Albar JP, et al. 1999. Fusogenic activity of hepadnavirus peptides corresponding to sequences downstream of the putative cleavage site. *Virology* 261(1):133–42

127. Poisson F, Severac A, Hourioux C, Goudeau A, Roingeard P. 1997. Both pre-S1 and S domains of hepatitis B virus envelope proteins interact with the core particle. *Virology* 228(1):115–20
128. Löffler-Mary H, Dumortier J, Klentsch-Zimmer C, Prange R. 2000. Hepatitis B virus assembly is sensitive to changes in the cytosolic S loop of the envelope proteins. *Virology* 270(2):358–67
129. Bruss V, Vieluf K. 1995. Functions of the internal pre-S domain of the large surface protein in hepatitis B virus particle morphogenesis. *J. Virol.* 69(11):6652–57
130. Schittl B, Bruss V. 2014. Mutational profiling of the variability of individual amino acid positions in the hepatitis B virus matrix domain. *Virology* 458:183–89
131. Koschel M, Oed D, Gerelsaikhan T, Thomssen R, Bruss V. 2000. Hepatitis B virus core gene mutations which block nucleocapsid envelopment. *J. Virol.* 74(1):1–7
132. Ponsel D, Bruss V. 2003. Mapping of amino acid side chains on the surface of hepatitis B virus capsids required for envelopment and virion formation. *J. Virol.* 77(1):416–22
133. Pairan A, Bruss V. 2009. Functional surfaces of the hepatitis B virus capsid. *J. Virol.* 83(22):11616–23
134. Dyson MR, Murray K. 1995. Selection of peptide inhibitors of interactions involved in complex protein assemblies: association of the core and surface antigens of hepatitis B virus. *PNAS* 92(6):2194–98
135. Böttcher B, Tsuji N, Takahashi H, Dyson MR, Zhao S, et al. 1998. Peptides that block hepatitis B virus assembly: analysis by cryomicroscopy, mutagenesis and transfection. *EMBO J.* 17(23):6839–45
136. Tan WS, Dyson MR, Murray K. 1999. Two distinct segments of the hepatitis B virus surface antigen contribute synergistically to its association with the viral core particles. *J. Mol. Biol.* 286(3):797–808
137. Tan WS. 2002. Inhibition of hepatitis B virus assembly with synthetic peptides derived from the viral surface and core antigens. *J. Gen. Appl. Microbiol.* 48(2):103–7
138. Pastor F, Herrscher C, Patient R, Eymieux S, Moreau A, et al. 2019. Direct interaction between the hepatitis B virus core and envelope proteins analyzed in a cellular context. *Sci. Rep.* 9(1):16178
139. Summers J, Mason WS. 1982. Replication of the genome of a hepatitis B–like virus by reverse transcription of an RNA intermediate. *Cell* 29(2):403–15
140. Scotto J, Hadchouel M, Wain-Hobson S, Sonigo P, Courouce AM, et al. 1985. Hepatitis B virus DNA in Dane particles: evidence for the presence of replicative intermediates. *J. Infect. Dis.* 151(4):610–17
141. Gerelsaikhan T, Tavis JE, Bruss V. 1996. Hepatitis B virus nucleocapsid envelopment does not occur without genomic DNA synthesis. *J. Virol.* 70(7):4269–74
142. Yuan TT, Sahu GK, Whitehead WE, Greenberg R, Shih C. 1999. The mechanism of an immature secretion phenotype of a highly frequent naturally occurring missense mutation at codon 97 of human hepatitis B virus core antigen. *J. Virol.* 73(7):5731–40
143. Yuan TT, Tai PC, Shih C. 1999. Subtype-independent immature secretion and subtype-dependent replication deficiency of a highly frequent, naturally occurring mutation of human hepatitis B virus core antigen. *J. Virol.* 73(12):10122–28
144. Yuan TT, Shih C. 2000. A frequent, naturally occurring mutation (P130T) of human hepatitis B virus core antigen is compensatory for immature secretion phenotype of another frequent variant (I97L). *J. Virol.* 74(10):4929–32
145. Le Pogam S, Shih C. 2002. Influence of a putative intermolecular interaction between core and the pre-S1 domain of the large envelope protein on hepatitis B virus secretion. *J. Virol.* 76(13):6510–17
146. Wu SY, Chang YS, Chu TH, Shih C. 2019. Persistence of hepatitis B virus DNA and the tempos between virion secretion and genome maturation in a mouse model. *J. Virol.* 93(22):e01001-19
147. Böttcher B, Nassal M. 2018. Structure of mutant hepatitis B core protein capsids with premature secretion phenotype. *J. Mol. Biol.* 430(24):4941–54
148. Nassal M. 1992. The arginine-rich domain of the hepatitis B virus core protein is required for pregenome encapsidation and productive viral positive-strand DNA synthesis but not for virus assembly. *J. Virol.* 66(7):4107–16
149. Schormann W, Kraft A, Ponsel D, Bruss V. 2006. Hepatitis B virus particle formation in the absence of pregenomic RNA and reverse transcriptase. *J. Virol.* 80(8):4187–90
150. Ning X, Nguyen D, Mentzer L, Adams C, Lee H, et al. 2011. Secretion of genome-free hepatitis B virus—single strand blocking model for virion morphogenesis of para-retrovirus. *PLOS Pathog.* 7(9):e1002255

151. Luckenbaugh L, Kitrinos KM, Delaney WE, Hu J. 2015. Genome-free hepatitis B virion levels in patient sera as a potential marker to monitor response to antiviral therapy. *J. Viral Hepat.* 22(6):561–70
152. Ning X, Basagoudanavar SH, Liu K, Luckenbaugh L, Wei D, et al. 2017. Capsid phosphorylation state and hepadnavirus virion secretion. *J. Virol.* 91(9):e00092-17
153. Hu J, Liu K. 2017. Complete and incomplete hepatitis B virus particles: formation, function, and application. *Viruses* 9(3):56
154. Ning X, Luckenbaugh L, Liu K, Bruss V, Sureau C, Hu J. 2018. Common and distinct capsid and surface protein requirements for secretion of complete and genome-free hepatitis B virions. *J. Virol.* 92(14):e00272-18
155. Gerin JL, Ford EC, Purcell RH. 1975. Biochemical characterization of Australia antigen. Evidence for defective particles of hepatitis B virus. *Am. J. Pathol.* 81(3):651–68
156. Kaplan PM, Ford EC, Purcell RH, Gerin JL. 1976. Demonstration of subpopulations of Dane particles. *J. Virol.* 17(3):885–93
157. Alberti A, Diana S, Scullard GH, Eddleston WF, Williams R. 1978. Full and empty Dane particles in chronic hepatitis B virus infection: relation to hepatitis B e antigen and presence of liver damage. *Gastroenterology* 75(5):869–74
158. Sakamoto Y, Yamada G, Mizuno M, Nishihara T, Kinoyama S, et al. 1983. Full and empty particles of hepatitis B virus in hepatocytes from patients with HBsAg-positive chronic active hepatitis. *Lab. Invest.* 48(6):678–82
159. Takahashi T, Kaga K, Akahane Y, Yamashita T, Miyakawa Y, Mayumi M. 1980. Isolation of Dane particles containing a DNA strand by metrizamide density gradient. *J. Med. Microbiol.* 13(1):163–66
160. Kimura T, Ohno N, Terada N, Rokuhara A, Matsumoto A, et al. 2005. Hepatitis B virus DNA-negative Dane particles lack core protein but contain a 22-kDa precore protein without C-terminal arginine-rich domain. *J. Biol. Chem.* 280(23):21713–19
161. Garcia PD, Ou JH, Rutter WJ, Walter P. 1988. Targeting of the hepatitis B virus precore protein to the endoplasmic reticulum membrane: After signal peptide cleavage translocation can be aborted and the product released into the cytoplasm. *J. Cell Biol.* 106(4):1093–104
162. Ou JH, Yeh CT, Yen TS. 1989. Transport of hepatitis B virus precore protein into the nucleus after cleavage of its signal peptide. *J. Virol.* 63(12):5238–43
163. Guidotti LG, Matzke B, Pasquinelli C, Shoenberger JM, Rogler CE, Chisari FV. 1996. The hepatitis B virus (HBV) precore protein inhibits HBV replication in transgenic mice. *J. Virol.* 70(10):7056–61
164. Scaglioni PP, Melegari M, Wands JR. 1997. Posttranscriptional regulation of hepatitis B virus replication by the precore protein. *J. Virol.* 71(1):345–53
165. Duriez M, Rossignol JM, Sitterlin D. 2008. The hepatitis B virus precore protein is retrotransported from endoplasmic reticulum (ER) to cytosol through the ER-associated degradation pathway. *J. Biol. Chem.* 283(47):32352–60
166. DiMattia MA, Watts NR, Stahl SJ, Grimes JM, Steven AC, et al. 2013. Antigenic switching of hepatitis B virus by alternative dimerization of the capsid protein. *Structure* 21(1):133–42
167. Duriez M, Thouard A, Bressanelli S, Rossignol JM, Sitterlin D. 2014. Conserved aromatic residues of the hepatitis B virus Precore propeptide are involved in a switch between distinct dimeric conformations and essential in the formation of heterocapsids. *Virology* 462:273–82
168. Eren E, Watts NR, Dearborn AD, Palmer IW, Kaufman JD, et al. 2018. Structures of hepatitis B virus core- and e-antigen immune complexes suggest multi-point inhibition. *Structure* 26(10):1314–26
169. Watts NR, Palmer IW, Eren E, Steven AC, Wingfield PT. 2020. Capsids of hepatitis B virus e antigen with authentic C termini are stabilized by electrostatic interactions. *FEBS Lett.* 594:1052–61
170. Tu T, Budzinska MA, Vondran FWR, Shackel NA, Urban S. 2018. Hepatitis B virus DNA integration occurs early in the viral life cycle in an *in vitro* infection model via sodium taurocholate cotransporting polypeptide-dependent uptake of enveloped virus particles. *J. Virol.* 92(11):e02007-17
171. Budzinska MA, Shackel NA, Urban S, Tu T. 2018. Cellular genomic sites of hepatitis B virus DNA integration. *Genes* 9(7):E365
172. Hallez C, Li X, Suspene R, Thiers V, Bouzidi MS, et al. 2019. Hypoxia-induced human deoxyribonuclease I is a cellular restriction factor of hepatitis B virus. *Nat. Microbiol.* 4(7):1196–207

173. Gilbert RJ, Beales L, Blond D, Simon MN, Lin BY, et al. 2005. Hepatitis B small surface antigen particles are octahedral. *PNAS* 102(41):14783–88
174. Dryden KA, Wieland SF, Whitten-Bauer C, Gerin JL, Chisari FV, Yeager M. 2006. Native hepatitis B virions and capsids visualized by electron cryomicroscopy. *Mol. Cell* 22(6):843–50
175. Seitz S, Urban S, Antoni C, Bottcher B. 2007. Cryo-electron microscopy of hepatitis B virions reveals variability in envelope capsid interactions. *EMBO J.* 26(18):4160–67
176. Short JM, Chen S, Roseman AM, Butler PJ, Crowther RA. 2009. Structure of hepatitis B surface antigen from subviral tubes determined by electron cryomicroscopy. *J. Mol. Biol.* 390(1):135–41
177. Cao J, Zhang J, Lu Y, Luo S, Zhang J, Zhu P. 2019. Cryo-EM structure of native spherical subviral particles isolated from HBV carriers. *Virus Res.* 259:90–96
178. Satoh O, Imai H, Yoneyama T, Miyamura T, Utsumi H, et al. 2000. Membrane structure of the hepatitis B virus surface antigen particle. *J. Biochem.* 127(4):543–50
179. Crowther RA. 2008. The Leeuwenhoek lecture 2006. Microscopy goes cold: Frozen viruses reveal their structural secrets. *Philos. Trans. R. Soc. B* 363(1502):2441–51
180. Leistner CM, Gruen-Bernhard S, Glebe D. 2008. Role of glycosaminoglycans for binding and infection of hepatitis B virus. *Cell Microbiol.* 10(1):122–33
181. Schulze A, Gripon P, Urban S. 2007. Hepatitis B virus infection initiates with a large surface protein-dependent binding to heparan sulfate proteoglycans. *Hepatology* 46(6):1759–68